Study on tribological properties of new TiAl based self-lubricating alloys

IOP Conf. Series: Materials Science and Engineering **504** (2019) 012006 doi:10.1088/1757-899X/504/1/012006

Study on tribological properties of new TiAl based self-lubricating alloys

C Wang, L Y Yang*, S R Wang, X Z Feng and B Yan

School of Mechanical Engineering, University of Jinan, Jinan, 250022, China

Corresponding author and e-mail: L Y Yang, eo_yangly@ujn.edu.cn

Abstract. The alloys are based on Ti-45Al-5Nb, Added different contents of TiC, Y_2O_3 and 62% BaF_2-38%CaF_2 to prepared new TiAl-based self-lubricating Alloys with excellent mechanical properties, excellent tribological properties and light weight. Investigated flexural strengths, fracture toughness, hardness, and densities of different compositions TiAl based self-lubricating alloys, as well as the friction and wear characteristics at 600 ℃. The results show that the mechanical properties, tribological properties and physics of the new TiAl-based alloys are better with 5% TiC, 0.25% Y_2O_3, and 13% (62% BaF_2-38%CaF_2). The wear mechanism of the alloys is adhesive wear.

1. Introduction

TiAl-based alloys with high relative strength, low density, good mechanical properties and flame retardancy under high temperature condition. They are considered as the most promising new generation of high-temperature resistant materials with wide applications in aerospace, automotive and so on[1-3].However, the insufficient tribological properties at high temperatures severely restrict the applications of TiAl-based alloys. So, it is great significance to study and improve the friction and wear properties of TiAl alloys under high temperature[4-5].

Added proper amount of solid lubricants in Ti-Al alloys can effectively improve the tribological properties. It was found that the eutectic solid lubricants 62%BaF_2-38%CaF_2 (hereinafter referred to as BC) has good anti-friction above 600°C. Added solid lubricants, the physical and mechanical properties of alloys have been reduced to varying degrees, which have great impact on its carrying capacity. But added some hard particles in TiAl alloys can effectively improve the mechanical properties. TiC, Al_2O_3, SiC, etc. are often added in alloys. Among these hard materials, TiC particles have good compatibility and great strengthening with the TiAl alloys[6]. Refinement grains can also effectively improve the mechanical and tribological properties for alloys. The rare earth elements with special structure which make they have special mechanical properties. Added a trace amount of rare earth elements can effectively refine grains size and improve the microstructures of the TiAl alloys[7]. The study found that the mechanical properties of Y_2O_3 are the most stable[8], the TiAl alloys added micron-sized Y_2O_3 are better than those which with the same amount of Y.

Therefore, in this study, Ti-45Al-5Nb as the matrix, added different amounts of Y_2O_3/TiC/BC to prepare new TiAl-based alloys with excellent mechanical properties, good wear resistances and self-lubricating properties. Study the mechanical and tribological properties of these alloys.

2. Alloys preparation

The raw materials used in experiments were Ti powders, Al powders, Nb powders, TiC powders, Y_2O_3 powders, BaF_2 powders, and CaF_2 powders. Among them, the purities of Ti, Al, Nb, BaF_2, CaF_2 are higher than 99.5%, the average particle sizes are less than 325 mesh; the purities of TiC and Y_2O_3 are 99.99%, and the average particle sizes are less than 50nm.

To Ti45Al5Nb matrix added different levels of TiC/Y_2O_3/BC, the percentages of different materials as shown in table 1. Here, using orthogonal experiment to match material compositions. The weighed powders were placed in a ball mill barrel, 200 r/min and ball milled for 4 h in argo. Then put those powders into the graphite mold, cold pressure molding under 30MPa for 1 min. Finally, the new TiAl-based self-lubricating alloys were prepared by vacuum hot-press sintering. The sintering process parameters are shown in table 2.

Table 1. Compositions of TiC/Y_2O_3/BC.

Materials / Level	Y_2O_3 (wt%) A	TiC (wt%) B	BC (wt%) C
1	0	0	7
2	0.25	2.5	10
3	0.5	5	13
4	0.75	7.5	15

Table 2. Sintering process parameters.

Temperature/□	Pressure/Mpa	Time/min
1200	30	30

3. Experimental results and discussion

3.1. Physical and mechanical properties of the samples

The bending strength, fracture toughness, actual density, and hardness test results of each component alloys are shown in table 3.

In the above tests, there are several test results for each sample. In order to analysis these results, quantify different indicators by comprehensive scores. Weighted by importance of different test results, the weights about bending strength: fracture toughness: hardness: the density are 3:3:2:2. Respectively, the comprehensive score is:

Comprehensive score = 3 × flexural strength + 3 × fracture toughness + 2 × hardness + 2 × density

According to the table 3, the largest range is factor B, factor C is second and factor A is last. So it can be seen that the degree of influence about the physical and mechanical properties were TiC, BC, Y_2O_3 in descending order. When B3C3A2 that 5% TiC, 13% BC, 0.25%Y_2O_3 the alloy is better. However, this alloy was not included in the above-mentioned 16 components. It is necessary to prepare this, which is numbered as 17, and compared with the above-mentioned 16 groups of samples.

According to the test results, the flexural strength, fracture toughness, hardness and density of No. 17 TiAl-based self-lubricating alloy is 522MPa, 13MPa $m^{1/2}$, 530HV, and 4.1g/cm^3. The Comprehensive score is 2682.89. As shown in figure1, No. 17 has the highest score, so No. 17 has the better comprehensive mechanical properties.

Table 3. Test results of samples.

Factors / Level	1 A	2 B	3 C	Various indicators experimental results				comprehensive score
				Flexural strength (MPa)	Fracture toughness ($MPam^{1/2}$)	Density (g/cm^3)	Hardness (HV)	
1	1	1	1	427	10.3	3.978	436.07	2191.99
2	1	2	2	475	11.6	3.921	498.13	2463.90
3	1	3	3	493	12.1	3.910	509	2541.12
4	2	4	4	461	11.2	3.833	458.3	2340.87
5	2	1	2	452.5	11.7	3.931	465.9	2332.26
6	2	2	1	464	11.4	4.025	492.25	2418.75
7	2	3	4	506	13.5	3.968	471.55	2509.54
8	2	4	3	523	14.2	3.926	482.23	2583.90
9	3	1	3	470	12.2	3.903	428.18	2310.76
10	3	2	4	454	14.6	3.959	457.33	2328.37
11	3	3	1	514	11.2	3.993	528.4	2640.39
12	3	4	2	444	10.6	3.967	547.55	2466.83
13	4	1	4	387	10.8	3.897	467.9	2136.99
14	4	2	3	490	12.2	3.964	430.9	2376.33
15	4	3	2	457	10.4	3.917	484.83	2379.69
16	4	4	1	458	12.5	3.927	542.06	2503.47
K1	9537.88	8972.01	9754.61					
K2	9844.45	9587.35	9642.69					
K3	9746.34	10070.74	9812.11					
K4	9396.49	9895.08	9315.76					
k1	2384.47	2243.00	2438.65					
k2	2461.11	2396.83	2410.67					
k3	2436.57	2517.68	2453.03					
k4	2349.12	2473.77	2328.94					
Range	111.99	274.68	124.09					
Excellent solution	A2	B3	C3					

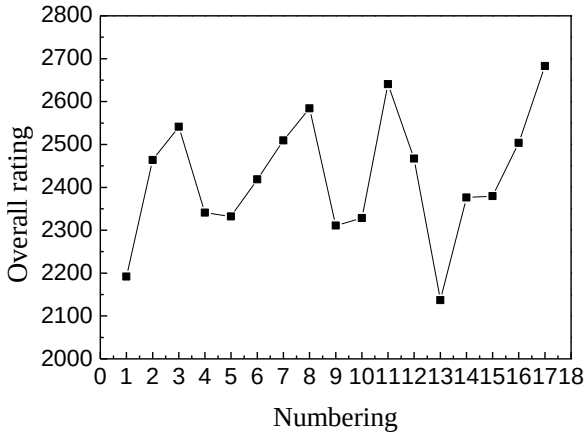

Figure 1. 17 samples comprehensive scores.

3.2. Samples fracture analysis

Figure 2(a) is a micrograph of the fracture surface of No.7, figure 2(b) is a microscopic topography of

the fracture surface of No.8 and figure 2(c) is a microscopic topography of the fracture surface of No.17.From figures 2(a)(b)(c), the fractures of the three alloys are very flat and these are typically brittle fractures. Figure 2(c) shows some strip morphologies at the fracture, which is typical transgranular cleavage fracture. This fracture means the alloys have good mechanical properties, especially the fracture toughness.

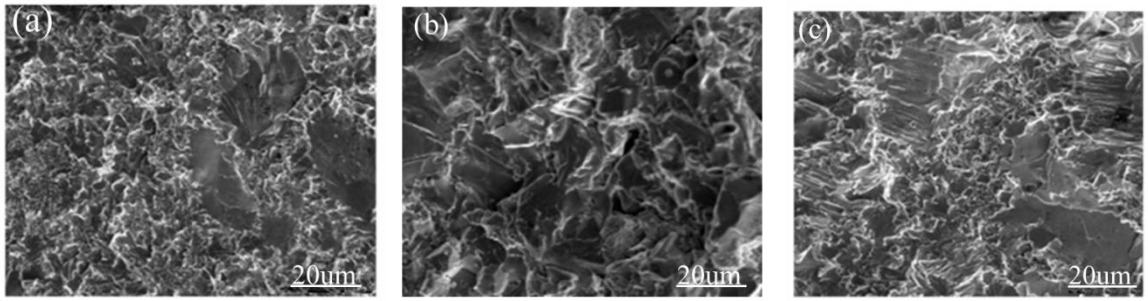

Figure 2. No.7, No.8, No.17 samples microcosmic fracture morphology.

3.3. The friction coefficient and wear rate of the samples

Under the conditions of 600°C, spindle speed 100r/min and load 100N, 17 groups of new TiAl-based self-lubricating alloys tested the changes about friction coefficient and wear rate. The test time is 60min.

Figure 3 shows the changes of friction coefficients and wear rates of 17 samples. It can be seen that the friction coefficients are between 0.28~0.44, the wear rates are between $0.27\times10^{-4}mm^{-3}N^{-1}m^{-1}$~$0.38\times10^{-4}mm^{-3}N^{-1}m^{-1}$. It is difficult to see the rule in figure 3, so further data processing is required.

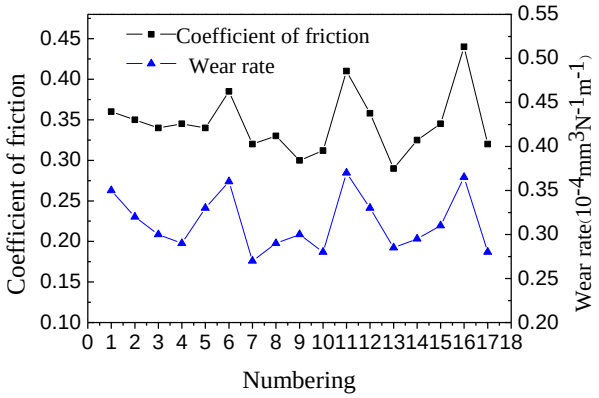

Figure 3. The change of friction coefficient and wear rate of 17 samples.

The 17 samples were divided into 4 groups based on the content of the self-lubricants, as shown in figures 4(a)(b)(c)(d). Figure 4(a) is the curves of the friction coefficients and the wear rates about samples at 7% BC, figure 4(b) is the curves of the friction coefficients and the wear rates about samples at 10% BC, figure 4(c) is the curves of the friction coefficients and the wear rates about samples at 13% BC, figure 4(d) is the curves of the friction coefficients and the wear rates about samples at 15% BC.

The samples numbers in figure 4(a) are 1,6,11 and 16, the friction coefficients are between 0.36~0.44, and the wear rates are between $0.32\times10^{-4}mm^{-3}N^{-1}m^{-1}$~$0.36\times10^{-4}mm^{-3}N^{-1}m^{-1}$, but No. 16 the wear rate has some decreased. With the hard particles TiC increased at certain extent the wear resistance has some effectively improved. Figure 4(b) are 2,5,12,15, the friction coefficients between 0.34~0.36, and the wear rates between $0.31\times10^{-4}mm^{-3}N^{-1}m^{-1}$~$0.33\times10^{-4}mm^{-3}N^{-1}m^{-1}$. Figure 4(c) are

3,8,9,14,17, the friction coefficients between 0.305~0.344, the wear rates between $0.28\times10^{-4}mm^{-3}N^{-1}m^{-1}$ ~$0.3\times10^{-4}mm^{-3}N^{-1}m^{-1}$. Figure 4(d) are 4,7,10,13, the friction coefficients between 0.29~0.34, and the wear rates between $0.27\times10^{-4}mm^{-3}N^{-1}m^{-1}$~$0.29\times10^{-4}mm^{-3}N^{-1}m^{-1}$. As the solid lubricants increase, the friction coefficients and wear rates of the alloys continue to decrease. Among them, the best friction and wear performance is No.13, and the friction coefficient and the wear rate is 0.29 and $0.285\times10^{-4}mm^{-3}N^{-1}m^{-1}$, but its mechanical ability is so poor. The friction coefficient is 0.32 and the wear rate is $0.283\times10^{-4}mm^{-3}N^{-1}m^{-1}$about No.17 with the better mechanical properties, which has better tribological properties than the other 16 specimens.

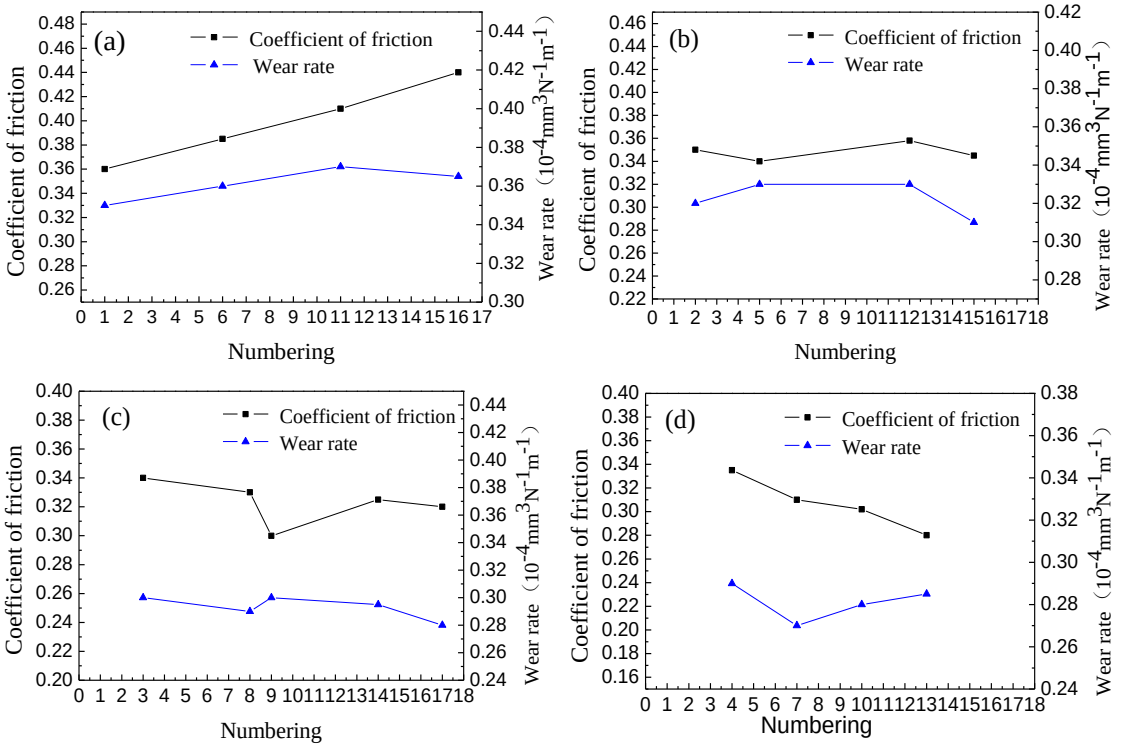

Figure 4 (a)(b)(c)(d). Curves of friction coefficients and wear rates of samples with different contents of solid lubricants.

3.4. Samples wear mechanism

Figure 5(a) is the No. 7 sample SEM image of surface abrasion, figure 5(b) is the No. 8 sample SEM image of surface abrasion, and Figure 5(c) is the No.17 sample SEM image of surface abrasion. It can be seen from figures 5(a)(b)(c), the wear patterns of the samples are adhesive wear. The figure 5(a)(b) show that there are some pits like a,b on the wear surface, and accompanied with some trace furrows. The reason is that as the temperature continues to rise in the wear surface, the solid lubricants BC expand and were pushed out. Under the continuous action of the abrasive parts, cracks appear at the position where the solid lubricants were extruded on the surface, forming fatigue and falling off, finally generating pits. Figure 5(c) shows the wear surface is relatively flat and there are no defects. Figure 6 is No.17 Wear Surface EDS, there are lots of Ba and Ca appear on the wear surface. This proves that No. 17 sample has excellent tribological properties and good self-lubricating properties on its friction surface.

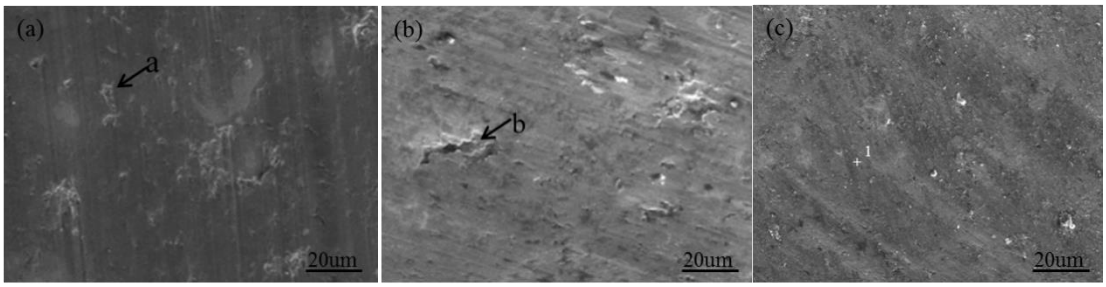

Figure 5. No.7, No.8, No.17 Wear Surface SEM.

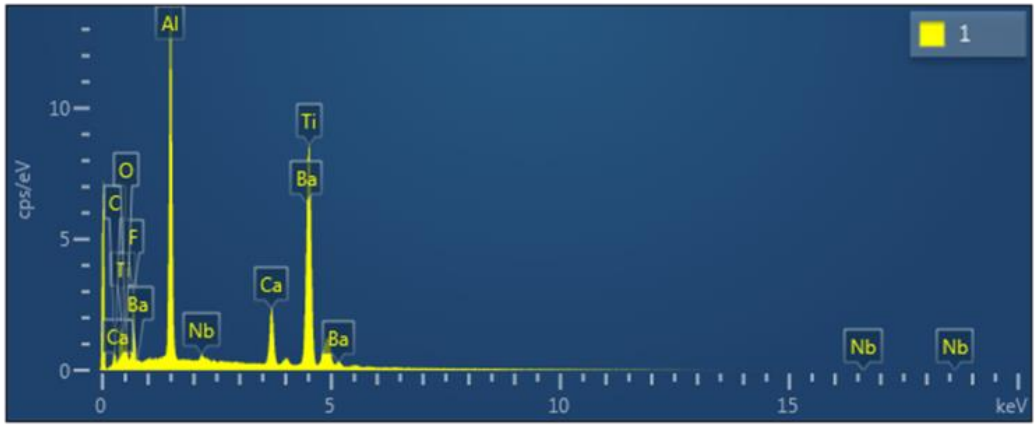

Figure 6. No.17 Wear Surface EDS.

Figures 7(a)(b)(c)(d) show the friction and wear processes of the samples. Figure 7(a) is the schematic diagram of the new TiAl self-lubricating alloy materials. TiC, Y_2O_3 and BC are randomly and uniformly distributed in the matrix. In the initial stages of friction and wear, solid lubricants do not fully function, when a portion of hard particles TiC are distributed on the wear surface, as shown in figure 7(b), the friction coefficient fluctuates has slightly and rises. But with the progress of friction and wear, the temperature keeps rising, solid lubricants BC were expand and extruded onto the wear surface as shown in figure (c). With the continuous rotation of the abrasive parts, the solid lubricants will spread evenly to the friction surface and as the solid lubricant continuously extruded, the complete lubricating film will be formed as shown in figure 7(d). At this time, the influence of the hard particles on the friction coefficient will be reduced, and the friction coefficient and wear rate will be decrease and tend to be stable.

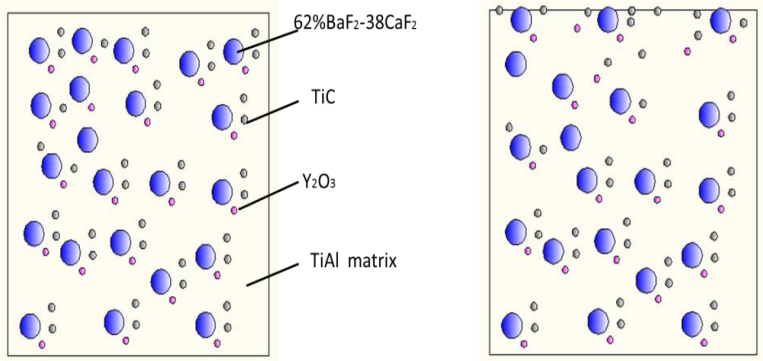

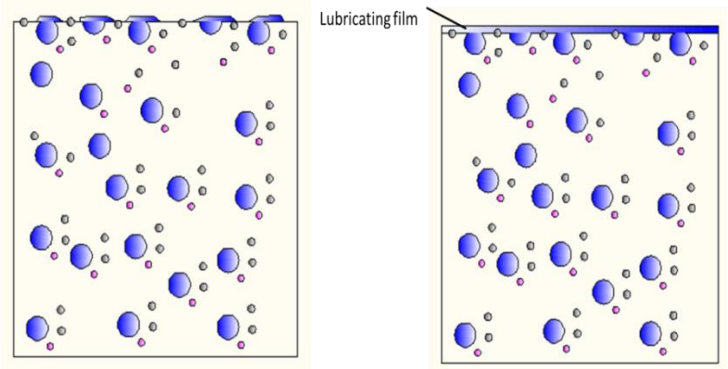

Figure 7. Lubrication mechanism of TiAl-based self-lubricating materials.

4. Conclusions

It was found that the new TiAl-based self-lubricating alloy with 5% TiC, 0.25% Y_2O_3, and 13% (62% BaF_2-38%CaF_2), the flexural strength, fracture toughness, hardness, and density were 522 MPa, 13 MPa $m^{1/2}$, 530 HV, 4.1 g/cm^3. At 600°C, 100N, 100r/mim and dry friction, the friction coefficient is 0.32, the wear rate is $0.283\times10^{-4}mm^{-3}N^{-1}m^{-1}$.Compared with other TiAl-based self-lubricating alloy materials, it has superior comprehensive performance.

With the increase of solid lubricant 62%BaF_2-38%CaF_2, the friction coefficient and wear rate have gradually decrease. The wear patterns of new TiAl-based alloys wear are adhesive wear. It shows that the alloys have stable and complete lubricating film on the friction surface at 13% BC, and they have good tribological properties.

Acknowledgement

The authors thank Shandong Key R&D Program (2018JMRH0407) for supporting this work.

References

[1] Bewlay B P, Nag S, Suzuki A and Weimer M J 2016 TiAl alloys in commercial aircraft engines *High Temperature Technology (Materials at High Temperatures* vol 33*)* pp 549-559

[2] Clemens H and Mayer S 2013 Design, processing, microstructure, and applications of advanced intermetallic TiAl alloys *Adv. Eng. Mater* vol 15 pp 191–215

[3] Liss K D, Funakoshi K I, Dippenaar R, Higo Y J, Shiro A, Reid M, Suzuki H, Shobu T and Akita K C 2016 Hydrostatic compression behavior and high-pressure stabilized β-phase in γ-based titanium aluminide intermetallics *Metals (Metallurgy* vol 6*)* p165

[4] Cheng J, Yang J, Zhang X H, Zhong H, Ma J Q, Li F, Fu L C, Bi Q L and Li J S 2012 High temperature tribological behavior of a Ti-46Al-2Cr-2Nb intermetallics *Intermetallics* vol 31(4) pp 120-126

[5] Rakesh K G and Suresh K R N 2017 Evaluation of friction and wear characteristics of electrostatic solid lubricant at different sliding conditions *Surface & Coatings Technology* vol 332 pp 341-350

[6] Nathan M and Ahearn J S 1993 Nanometre-scale chemical compatibility of TiAl with Al_2O_3, TiB_2 and TiC *Materials Science Letters* vol 12(20) pp1622-1624

[7] Ma X Z, Shen J and Jia J. 2001 Microstructure evolution of rare earth rich phase for rapidly-solidified TiAl based alloys *Materials Science Letters* pp 2013-2015

[8] Gao M, Cui R J, Ma L M, Zhang H R and Tang X X 2011 Physical erosion of yttria crucibles in Ti–54Al alloy casting process *Materials Processing Technology* vol 211(12) pp 2004-2011